Int. J. Heat Mass Transfer. Vol. 35, No. 9, pp. 2277–2287, 1992
Printed in Great Britain

0017–9310/92 $5.00 + 0.00
Pergamon Press Ltd

Numerical study of heat and mass transfer from an inclined flat plate with wet and dry zones

M. MAMMOU and M. DAGUENET
Laboratoire de Thermodynamique et Energétique, Université de Perpignan, Avenue de Villeneuve, 66025 Perpignan Cédex, France

and

G. LE PALEC
Université Aix Marseille II, E.S.M. 2, Institut Méditerranien de Technologie, Technopôle Chateau, Gombert, 13451 Marseille Cedex 13, France

(*Received* 14 *June* 1990 *and in final form* 15 *July* 1991)

Abstract—This paper presents a theoretical study of momentum, heat and mass transfer in the laminar boundary layer which develops over an inclined flat plate by either free or forced convection when a constant wall heat flux is specified: this plate is made with two wet zones which are separated by a dry one. From the theoretical analysis, a set of dimensionless coupled equations is deduced and numerically solved by using an implicit finite difference method. The results show the effect of most of the main physical quantities upon velocity, temperature and concentration profiles in the boundary layer: from this study, the length of the dry separation zone appears as an essential criterion.

1. INTRODUCTION

IN THE bulk of heat and mass transfer over plates by either natural, mixed or forced convection, many papers involving experimental and theoretical investigations have been published in the literature and most of these studies are based upon the laminar boundary layer approach [1–5]. It follows that this problem is now well known and the mathematical models and correlations which have been developed can be applied to many industrial processes, such as chemical and drying processes. For these models, a constant wall condition is generally specified, but there are processes for which this assumption is not justified. As an example, in wood dryers, it is possible that some pieces are already dry whereas others which are placed beside them stay wet. In this paper, we focus on this type of problem in order to show how the boundary layers which grow over the wet and dry zones can interact and also to illustrate the effects of this upon the local Nusselt and Sherwood numbers. For this purpose, a numerical procedure which can be applied to both forced and free convection cases has been developed. The geometry of the problem under consideration is shown in Fig. 1: a flat plate, with an inclination angle α from the vertical direction, is divided into three regions. The first and the third zones, with lengths x_1 and $(L-x_2)$ respectively, are wet and they are separated by a dry zone, the length of which is (x_2-x_1). The plate is plunged into a Newtonian fluid (air), which can either be at rest (free convection case) or have a constant velocity U_∞: in both cases and far from the wall, the temperature and concentration of the fluid are T_∞ and C_∞, respectively. A constant wall heat flux q is specified on the three regions, so that high variations in the wall temperature and concentration values occur at $x = x_1$ and $x = x_2$ because of the changes in evaporation conditions.

2. THEORETICAL ANALYSIS

2.1. *Simplifying assumptions*

In order to set the partial differential system of equations which describes momentum, heat and mass transfer in the boundary layer, some simplifying assumptions are necessary. First of all, we assume that the moist air is an ideal gas with constant physical properties except for its density, the variations of

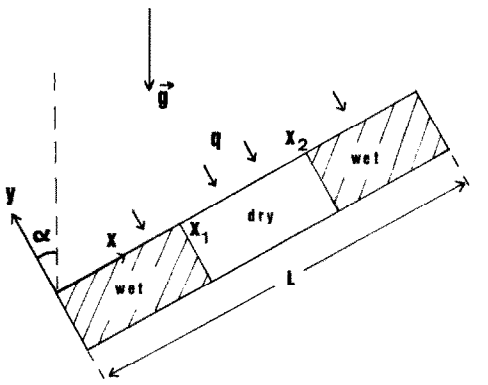

FIG. 1. Problem statement and definition of the coordinates.

NOMENCLATURE

C	vapour concentration in the boundary layer [kg kg^{-1}]
C^*	dimensionless vapour concentration in the boundary layer
C_0	dry air concentration in the wet air [kg kg^{-1}]
C_p	specific heat of the wet air [J kg^{-1} K^{-1}]
C_w	wall vapour concentration [kg kg^{-1}]
C_w^*	dimensionless wall vapour concentration
C_∞	vapour concentration far from the wall [kg kg^{-1}]
D	mass diffusion coefficient of vapour in dry air [m^2 s^{-1}]
g	gravitational acceleration [m s^{-2}]
Gr_L^*	modified Grashof number defined by equation (16)
L	length of the plate along the x direction [m]
L_T	vaporization latent heat of water [J kg^{-1}]
Nu_x	local Nusselt number
P	atmospheric pressure [N m^{-2}]
P_{vs}	partial pressure of saturated vapour on the wall [N m^{-2}]
Pr	Prandtl number: $Pr = \mu C_p/\lambda$
q	incident heat flux per unit area [W m^{-2}]
Re	Reynolds number, defined in equation (17)
Sc	Schmidt number: $Sc = \nu/D$
Sh_x	local Sherwood number
T	temperature in the boundary layer [K]
T^*	dimensionless temperature in the boundary layer
T_w	wall temperature [K]
T_w^*	dimensionless wall temperature
T_∞	temperature of the fluid far from the wall [K]
u	velocity component in the x direction [m s^{-1}]
u^*	dimensionless velocity component in the x^* direction
U_∞	velocity of the forced flow (forced convection case) [m s^{-1}]
v	velocity component in the y direction [m s^{-1}]
v^*	dimensionless velocity component in the y^* direction
x, y	coordinates shown in Fig. 1 [m]
x^*, y^*	dimensionless coordinates defined in Table 1
x_1, x_2	coordinates of the separation zones as shown in Fig. 1 [m]
x_1^*, x_2^*	dimensionless values of x_1 and x_2.

Greek symbols

α	inclination angle from the vertical direction [rad]
β	coefficient of thermal expansion [K^{-1}]
β^*	coefficient of mass expansion [kg kg^{-1}]
$\delta(x)$	local thickness of the boundary layer [m]
ε	constant factor: $\varepsilon = 1$ for the free convection case and $\varepsilon = 0$ for the forced convection case
Γ_x	local wall shear stress divided by ρ: $\Gamma_x = \nu\,\partial u/\partial y\|_{y=0}$ [m^2 s^{-2}]
λ	thermal conductivity of the fluid [W m^{-1} K^{-1}]
μ	dynamic viscosity of the fluid [kg m^{-1} s^{-1}]
ν	kinematic viscosity of the fluid [m^2 s^{-1}]
ρ	density of the fluid [kg m^{-3}].

which are possibly at the origin of free convection. In the case of natural convective flow, the Boussinesq approximation is retained and the inclination angle of the plate, α, is restricted to the following condition [6]:

$$\frac{\delta(x)}{x}\tan(\alpha) \ll 1 \tag{1}$$

where x is the distance measured along the wall from the stagnation point (see Fig. 1) and $\delta(x)$ is the thickness of the boundary layer: this condition ensures that the pressure variation along the x direction is negligible.

Secondly, for the two wet zones, the moisture is assumed to be so high that the wall temperature T_w and vapour concentration C_w can be related through the wall saturated pressure P_{vs}, accordingly to the following equation:

$$C_w(T_w) = 0.622\frac{P_{vs}}{P - 0.378P_{vs}} \tag{2}$$

where P is the total (atmospheric) pressure and P_{vs} is evaluated from the Bertrand formula [7]:

$$P_{vs} = 10^{(17.443 - 2795/T_w - 3.868\log_{10}(T_w))}. \tag{3}$$

Lastly, it is assumed that the vapour coming from the wall does not disrupt the flow. Other classical assumptions such as steady state flow, negligible viscous dissipation, thermodiffusion and radiative effects are also retained.

2.2. *Governing equations*

Let u and v be the velocity components along the x and y axes, respectively, T and C being the temperature and vapour concentration in the boundary layer. The governing equations which correspond to

the above assumptions are:

$$\frac{\partial u}{\partial x}+\frac{\partial v}{\partial y}=0 \tag{4}$$

$$u\frac{\partial u}{\partial x}+v\frac{\partial v}{\partial y}=v\frac{\partial^2 u}{\partial y^2}+\varepsilon g\cos(\alpha)[\beta(T-T_\infty)+\beta^*(C-C_\infty)] \tag{5}$$

$$u\frac{\partial T}{\partial x}+v\frac{\partial T}{\partial y}=\frac{\lambda}{\rho C_p}\frac{\partial^2 T}{\partial y^2} \tag{6}$$

$$u\frac{\partial C}{\partial x}+v\frac{\partial C}{\partial y}=D\frac{\partial^2 C}{\partial y^2} \tag{7}$$

where $\varepsilon = 1$ for the natural convection case and $\varepsilon = 0$ for the forced convection case. In equation (5), g is the gravitational acceleration, ν is the kinematic viscosity of the moist air, and β and β^* are, respectively, the coefficient of thermal expansion and the coefficient of mass expansion. The other physical quantities appearing in equations (6) and (7) are defined in the Nomenclature. The differential system of equations (4)–(7) is subjected to wall conditions which are different for the wet zones than for the dry zone.

(i) For the wet zones ($x < x_1$ and $x > x_2$), the wall temperature and vapour concentration are related by equation (2); we also have

$$u(x,0)=0 \tag{8}$$

$$v(x,0)=-\frac{D}{1-C_0}\left.\frac{\partial C}{\partial y}\right|_{y=0} \tag{9}$$

$$q=-\lambda\left.\frac{\partial T}{\partial y}\right|_{y=0}-L_T\rho D\left.\frac{\partial C}{\partial y}\right|_{y=0}. \tag{10}$$

In equation (9), which is deduced from the Fick law [8], C_0 is the dry air concentration. As shown from equation (10), the constant wall heat flux q divides into two components, the last of which is the latent heat flux. In this equation, L_T is the vaporization latent heat of water; it can be evaluated from the following relation [7]:

$$L_T = 4185[579-0.56(T_w-273.15)]. \tag{11}$$

(ii) For the dry zone ($x_1 < x < x_2$), the normal wall velocity component and the wall vapour concentration are equal to zero because there is no evaporation. We thus have:

$$u(x,0)=v(x,0)=\left.\frac{\partial C}{\partial y}\right|_{y=0}=0 \tag{12}$$

$$q=-\lambda\left.\frac{\partial T}{\partial y}\right|_{y=0}. \tag{13}$$

For all cases and far from the wall, the boundary conditions are

$$u\to(1-\varepsilon)U_\infty;\quad v\to 0;\quad T\to T_\infty;\quad C\to C_\infty. \tag{14}$$

For $x = 0$, we have:

$$u=(1-\varepsilon)U_\infty;\quad T=T_\infty;\quad C=C_\infty. \tag{15}$$

2.3. *Dimensionless form of equations*

Equations (4)–(7) and boundary conditions (2) and (8)–(15) have been transformed by introducing the dimensionless coordinates x^* and y^* and the dimensionless form of the velocity components (u^* and v^*), temperature (T^*) and vapour concentration (C^*): the definitions of these quantities are given in Table 1 for both free and forced convection cases. In these definitions, Gr_L^* is the modified Grashof number which is defined by the following relation:

$$Gr_L^*=\frac{g\beta q\cos(\alpha)L^4}{\lambda\nu^2} \tag{16}$$

and the Reynolds number, Re, is

$$Re=\frac{U_\infty L}{\nu}. \tag{17}$$

Substitution of the definitions of Table 1 in the governing equations leads to the following differential system of dimensionless equations:

$$\frac{\partial u^*}{\partial x^*}+\frac{\partial v^*}{\partial y^*}=0 \tag{18}$$

$$u^*\frac{\partial u^*}{\partial x^*}+v^*\frac{\partial v^*}{\partial y^*}=\frac{\partial^2 u^*}{\partial y^{*2}}+\varepsilon(T^*+C^*) \tag{19}$$

$$u^*\frac{\partial T^*}{\partial x^*}+v^*\frac{\partial T^*}{\partial y^*}=\frac{1}{Pr}\frac{\partial^2 T^*}{\partial y^{*2}} \tag{20}$$

$$u^*\frac{\partial C^*}{\partial x^*}+v^*\frac{\partial C^*}{\partial y^*}=\frac{1}{Sc}\frac{\partial^2 C^*}{\partial y^{*2}} \tag{21}$$

where Pr and Sc are the Prandtl number and the Schmidt number, the definitions of which are given in

Table 1. Definition of dimensionless quantities

	Free convection case	Forced convection case
x^*	$\frac{x}{L}$	$\frac{x}{L}$
y^*	$\frac{y}{L}Gr_L^{*1/5}$	$\frac{y}{L}Re^{1/2}$
u^*	$\frac{uL}{\nu}Gr_L^{*-2/5}$	$\frac{u}{U_\infty}$
v^*	$\frac{vL}{\nu}Gr_L^{*-1/5}$	$\frac{v}{U_\infty}$
T^*	$\frac{g\cos(\alpha)\beta(T-T_\infty)}{\nu^2}L^3Gr_L^{*-4/5}$	$\frac{T}{T_\infty}$
C^*	$\frac{g\beta^*\cos(\alpha)(C-C_\infty)}{\nu^2}L^3Gr_L^{*-4/5}$	$\frac{C}{C_\infty}$

the Nomenclature. The boundary conditions become

(i) For the wet zones ($0 < x^* < x_1/L$ and $x_2/L < x^* < 1$)

$$u^*(x^*, 0) = 0 \tag{22}$$

$$v^*(x^*, 0) = -A_v \left.\frac{\partial C^*}{\partial y^*}\right|_{y^*=0} \tag{23}$$

$$\left.\frac{\partial T^*}{\partial y^*}\right|_{y^*=0} + A_T \left.\frac{\partial C^*}{\partial y^*}\right|_{y^*=0} = -B_T \tag{24}$$

$$C_w^* = \frac{C_w(T_w)}{C_\infty}. \tag{25}$$

In equations (23) and (24), the coefficients A_v, A_T and B_T are, for the free convection case

$$A_v = \frac{DLq\beta}{(1-C_0)\lambda\nu\beta^*} Gr_L^{*-1/5}; \quad A_T = \frac{L_T \rho D\beta}{\lambda\beta^*}; \quad B_T = 1$$

and for the forced convection case, these definitions are

$$A_v = \frac{DC_\infty Re^{1/2}}{U_\infty L(1-C_0)}; \quad A_T = \frac{L_T \rho D C_\infty}{\lambda T_\infty};$$

$$B_T = \frac{Lq}{\lambda T_\infty} Re^{-1/2}.$$

(ii) For the dry zone ($x_1^* < x^* < x_2^*$)

$$u^*(x^*, 0) = v^*(x^*, 0) = \left.\frac{\partial T^*}{\partial y^*}\right|_{y^*=0} + 1$$

$$= \left.\frac{\partial C^*}{\partial y^*}\right|_{y^*=0} = 0. \tag{26}$$

Far from the wall, the boundary conditions are

$$\begin{aligned} &u^*(x^*, \infty) \to 1-\varepsilon; \quad v^*(x^*, \infty) \to 0; \\ &T^*(x^*, \infty) \to 1-\varepsilon; \quad C^*(x^*, \infty) \to 1-\varepsilon \end{aligned} \tag{27}$$

and for $x^* = 0$, we get

$$u^*(0, y^*) = T^*(0, y^*) = C^*(0, y^*) = 1-\varepsilon. \tag{28}$$

Equations (18)–(21) and boundary conditions (22)–(28) were solved by using a numerical procedure which is described in the next section. The interesting physical quantities are the local Nusselt number (Nu_x), the local Sherwood number (Sh_x) and the local wall shear stress (Γ_x): their definitions are given in Table 2 for both free and forced convection cases.

Table 2. Definitions of local Nusselt and Sherwood numbers and local dimensionless local wall shear stress

	Free convection case	Forced convection case
Nu_x	$-Gr_L^{*1/5} \dfrac{x^* \left.\dfrac{\partial T^*}{\partial y^*}\right\|_{y^*=0}}{T^*(x^*, 0)}$	$-Re^{1/2} \dfrac{x^* \left.\dfrac{\partial T^*}{\partial y^*}\right\|_{y^*=0}}{T^*(x^*, 0)-1}$
Sh_x	$-Gr_L^{*1/5} \dfrac{x^* \left.\dfrac{\partial C^*}{\partial y^*}\right\|_{y^*=0}}{C^*(x^*, 0)}$	$-Re^{1/2} \dfrac{x^* \left.\dfrac{\partial C^*}{\partial y^*}\right\|_{y^*=0}}{C^*(x^*, 0)-1}$
Γ_x	$\dfrac{\nu^2}{L^2} Gr_L^{*3/5} \left.\dfrac{\partial u^*}{\partial y^*}\right\|_{y^*=0}$	$\dfrac{\nu U_\infty}{L} Re^{1/2} \left.\dfrac{\partial u^*}{\partial y^*}\right\|_{y^*=0}$

3. NUMERICAL PROCEDURE

The numerical procedure has been adapted from the method which was proposed by Nogotov [9]. For this purpose, the boundary layer region has been divided into rectangles of length Δx^* and width Δy^*. An upwind finite difference technique is used in order to discretize equations along the x^* direction, whereas central differences are applied for the first and second derivative approximations with respect to the y^* direction. Let i and j represent a grid point of the boundary layer: the resulting finite difference approximation of equations (18)–(21) is

$$v_{j+1}^{*i+1} = v_j^{*i+1} - \frac{\Delta y^*}{\Delta x^*}(u_j^{*i+1} - u_j^{*i}) \tag{29}$$

$$a_{1j}u_{j+1}^{*i+1} + b_{1j}u_j^{*i+1} + c_{1j}u_{j+1}^{*i+1} - \varepsilon(T_j^{*i+1} + C_j^{*i+1}) = d_{1j} \tag{30}$$

$$a_{2j}T_{j-1}^{*i+1} + b_{2j}T_j^{*i+1} + c_{2j}T_{j+1}^{*i+1} = d_{2j} \tag{31}$$

$$a_{3j}C_{j-1}^{*i+1} + b_{3j}C_j^{*i+1} + c_{3j}C_{j+1}^{*i+1} = d_{3j} \tag{32}$$

where

$$a_{kj} = -\frac{v_j^{*i}}{2\Delta y^*} - \frac{1}{A(\Delta y^*)^2};$$

$$b_{kj} = \frac{u_j^{*i}}{2\Delta x^*} + \frac{2}{A(\Delta y^*)^2};$$

$$c_{kj} = \frac{v_j^{*i}}{2\Delta y^*} - \frac{1}{A(\Delta y^*)^2};$$

$$d_{kj} = \frac{u_j^{*i} f_j^i}{\Delta x^*}$$

with:

$$\begin{aligned} &A = 1 \quad \text{and} \quad f_j^i = u_j^{*i} \quad \text{for} \quad k = 1; \\ &A = Pr \quad \text{and} \quad f_j^i = T_j^{*i} \quad \text{for} \quad k = 2; \\ &A = Sc \quad \text{and} \quad f_j^i = C_j^{*i} \quad \text{for} \quad k = 3. \end{aligned}$$

For the boundary conditions, a Taylor expansion is used in order to calculate the wall temperature and vapour concentration derivatives. For $y^* = 0$ (i.e. for $j = 1$), we have the following.

(i) For the two wet zones ($0 < x^* < x_1^*$ and $x_2^* < x^* < 1$)

$$u_1^{*i+1} = 0 \tag{33}$$

$$v_1^{*i+1} = A_v \frac{1}{2\Delta y^*}(3C_1^{*i+1} - 4C_2^{*i+1} + C_3^{*i+1}) \tag{34}$$

$$3T_1^{*i+1} - 4T_2^{*i+1} + T_3^{*i+1} + A_T(3C_1^{*i+1} - 4C_2^{*i+1} + C_3^{*i+1}) = 2\Delta y^* \tag{35}$$

$$C_1^{*i+1} = g(T_1^{*i+1}) \quad (36)$$

where the function $g(T^*)$ is defined from equation (25).

(ii) For the dry zone ($x_1^* < x^* < x_2^*$)

$$u_1^{*i+1} = v_1^{*i+1} = 0 \quad (37)$$

$$3T_1^{*i+1} - 4T_2^{*i+1} + T_3^{*i+1} = 2\Delta y^* \quad (38)$$

$$3C_1^{*i+1} - 4C_2^{*i+1} + C_3^{*i+1} = 0. \quad (39)$$

For $j = J$ (i.e. $y^* \to \infty$), the boundary conditions are

$$u_J^{*i+1} \to 1-\varepsilon; \quad v_J^{*i+1} \to 0,$$
$$T_J^{*i+1} \to 1-\varepsilon; \quad C_J^{*i+1} \to 1-\varepsilon. \quad (40)$$

Finally, for $i = 1$ and $j = J = 1$ (i.e. $x^* = 0$), we get

$$u_1^{*1} = T_1^{*1} = C_1^{*1} = 1-\varepsilon. \quad (41)$$

From the discretized system of equations (29)–(32), it is seen that each of them form a system of $(N \times J)$ linear algebraic equations (N being the number of grid points along the x^* direction). For each value of i ($i = 1$ to $N-1$), these equations are transformed into a matricial system which is solved by using a Gaussian elimination method [10, 11], the maximal value of j (i.e. J) being determined from the following additional boundary condition:

$$v\left.\frac{\partial u}{\partial y}\right|_{y\to\infty} \to 0, \quad (42)$$

the discretization of which gives

$$1-\varepsilon-u_{J-1}^{*i+1} \leqslant \varepsilon_u \quad (43)$$

where $\varepsilon_u \simeq 0$. The details of matricial calculations can be found in ref. [6] and will not be repeated here.

The numerical solution is obtained by first selecting, for $i = 1$, an arbitrary value for J and for the wall temperature T_1^{*2} from which the value of the wall vapour concentration is deduced by means of equation (36). The matricial system of equations can then be solved and a new value of the wall temperature, say θ_1^2, is determined and compared with the guessed value T_1^{*2}: if the temperature difference $|T_1^{*2} - \theta_1^2|$ is greater than a prefixed accuracy, the new starting value is obtained from

$$T_{1,\text{new}}^{*2} = \frac{T_{1,\text{old}}^{*2} + \theta_1^2}{2} \quad (44)$$

and the procedure is repeated. Once the desired accuracy is obtained, the additional boundary condition (42) is tested: if this condition is not verified, the value of J is incremented and the above calculations are repeated until equation (43) is satisfied. The same numerical procedure is then applied for $i = 2, \ldots, i = N-1$.

4. RESULTS AND DISCUSSION

All the results of this study have been carried out with $Pr = 0.71$ and $Sc = 0.63$. First, the mathematical model and numerical procedure have been tested by comparing our results with some particular cases which were reported in the literature. It has been verified that our results agree with those of Callahan and Marner [12] for the problem of free convection from an isothermal flat plate. This problem has also been treated by Bottemane [13] and Gebhart and Pera [14]. For the case of evaporation from a vertical plate subject to a uniform wall heat flux, the comparison between our results and those of Vachon [15] shows a good agreement, as can be seen from Table 3.

Table 3. Comparison between our results and those of ref. [15]

Reference [15]			Our results	
Gr_x^*	Nu_x	Sh_x	Nu_x	Sh_x
3.607×10^9	39.959	37.814	39.183	35.814
7.410×10^9	46.148	43.323	45.586	41.643
9.410×10^9	48.415	45.451	47.922	43.768
16.77×10^9	54.337	51.010	54.016	49.332

4.1. *Forced convection case*

For several distances from the wall, Figs. 2–4 show the dimensionless x-velocity component, temperature and vapour concentration profiles in the boundary layer. These results have been carried out with $x_1^* = x_1^* - x_2^* = 1 - x_2^* = 1/3$, $q = 300$ W m^{-2} and $U_\infty = 0.8$ m s^{-1}. The velocity is a decreasing function of x^* and its profile is not affected by the separation zones between the dry and the two wet regions, which is the consequence of $\varepsilon = 0$ in the momentum equation (5). On the other hand, the temperature and vapour concentration profiles are highly influenced by the presence of the dry zone: as can be seen from Fig. 3, the temperature increases with x^* in all the three

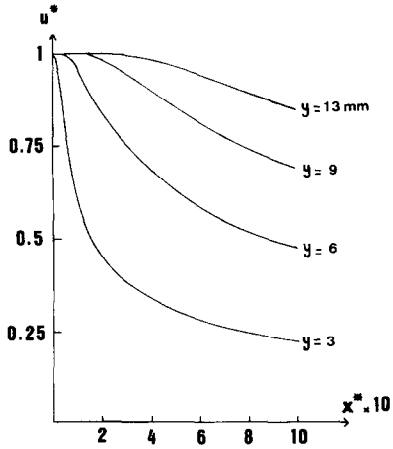

FIG. 2. Dimensionless x^*-velocity component profiles in the boundary layer: forced convection case. $T_\infty = 298$ K; $q = 300$ W m^{-2}; $C_\infty = 0.008$ kg kg^{-1} (dry basis); $U_\infty = 0.8$ m s^{-1}.

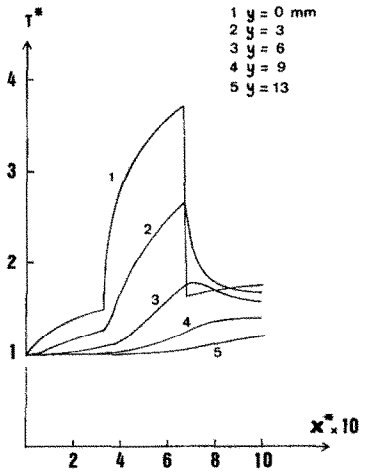

FIG. 3. Dimensionless temperature profiles in the boundary layer: forced convection case. $T_\infty = 298$ K; $q = 300$ W m^{-2}; $C_\infty = 0.008$ kg kg^{-1} (dry basis); $U_\infty = 0.8$ m s^{-1}.

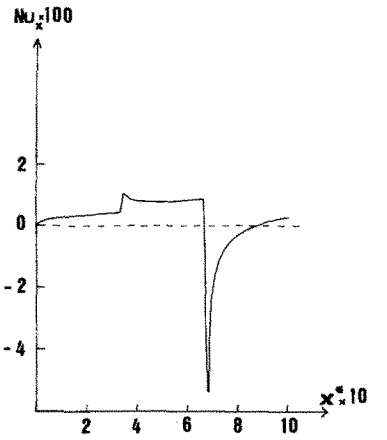

FIG. 5. Local Nusselt number as a function of x^*: forced convection case. $T_\infty = 298$ K; $q = 300$ W m^{-2}; $C_\infty = 0.008$ kg kg^{-1} (dry basis); $U_\infty = 0.8$ m s^{-1}.

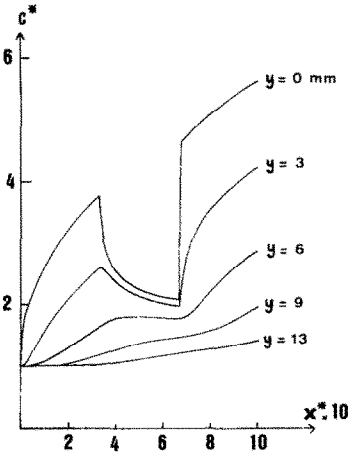

FIG. 4. Dimensionless vapour concentration profiles in the boundary layer: forced convection case. $T_\infty = 298$ K; $q = 300$ W m^{-2}; $C_\infty = 0.008$ kg kg^{-1} (dry basis); $U_\infty = 0.8$ m s^{-1}.

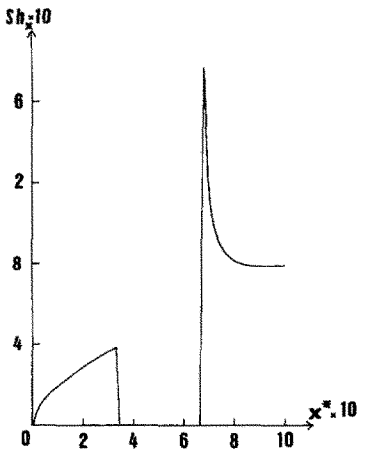

FIG. 6. Local Sherwood number as a function of x^*: forced convection case. $T_\infty = 298$ K; $q = 300$ W m^{-2}; $C_\infty = 0.008$ kg kg^{-1} (dry basis); $U_\infty = 0.8$ m s^{-1}.

regions, but this increase is larger along the dry zone because there is no evaporation process on the wall, so that the sensible heat is higher according to the thermal balances (10) and (13). From Fig. 4, it is seen that the vapour concentration is an increasing function of x^* in the two wet zones, whereas it decreases with x^* above the dry region.

As a result of these sudden variations in the wall temperature and vapour concentration values at the separation zones, the local Nusselt and Sherwood numbers are also discontinuous functions of x^*, as shown in Figs. 5 and 6. For the first moist region, the local Nusselt and Sherwood numbers increase with x^*. For $x^* > x_1^*$ and up to $x^* > x_2^*$, the Sherwood number becomes equal to zero, because there is no evaporation, and the wall temperature increase induced higher values of the local Nusselt number. At the very beginning of the second wet zone ($x^* = x_2^*$), the wall temperature is so high that the latent heat flux is much greater than the sensible heat flux, so that the local Nusselt number first becomes negative and then increases with x^*, again becoming positive at approximately $x^* = 0.9$. At the same time, the local Sherwood number first highly increases before decreasing and again increasing. It should be noted that a negative value of the local Nusselt number means that the heat passes from the drying air towards the plate. Figure 7 shows the variations of the local wall shear stress: as can be predicted from the velocity profile, it is a continuous decreasing function of x^*.

The effect of the length of the dry zone upon the local Nusselt and Sherwood numbers is shown in Figs. 8 and 9: for these calculations, the total length of the plate (L) is assumed to be equal to 1 m. For the points

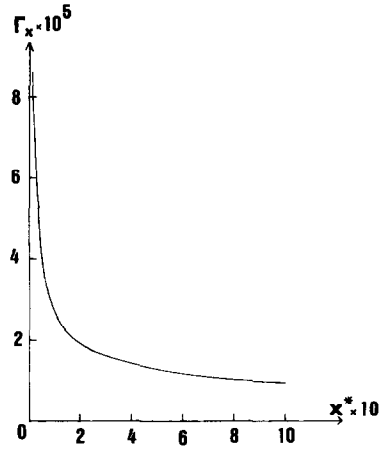

FIG. 7. Local wall shear stress as a function of x^*: forced convection case. $T_\infty = 298$ K; $q = 300$ W m^{-2}; $C_\infty = 0.008$ kg kg^{-1} (dry basis); $U_\infty = 0.8$ m s^{-1}.

located at $y = 3$ mm from the wall, the corresponding temperature and vapour concentration profiles are plotted in Figs. 10 and 11. It is seen that the larger the length $(x_2 - x_1)$, the higher the mass transfer rate and the lower the heat transfer rate along the second wet region are: this is due to the fact that an increasing value of the dry zone length produces a higher wall temperature with an accompanying increase of the wall partial pressure of saturated vapour for $x = x_2$. At the same time, an increasing value of $(x_2 - x_1)$ induces a decreasing relative humidity of the drying air, as can be seen from the dimensionless temperature and concentration profiles. As a result, the longer the dry zone length, the larger the evaporation rate for $x = x_2$.

Figures 12 and 13 show the variations of the local Nusselt and Sherwood numbers as a function of the velocity of the forced flow, U_∞: it is seen that the heat and mass transfer rates increase with this velocity

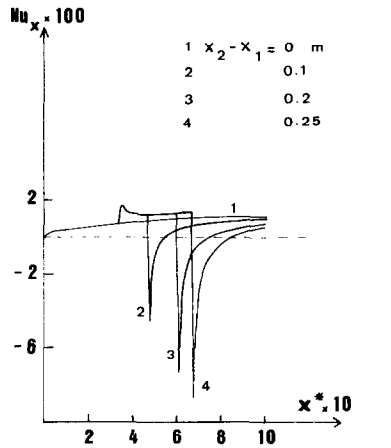

FIG. 8. Effect of the dry zone length on the local Nusselt number: forced convection case. $T_\infty = 298$ K; $q = 300$ W m^{-2}; $C_\infty = 0.008$ kg kg^{-1} (dry basis); $U_\infty = 2$ m s^{-1}; $L = 1$ m.

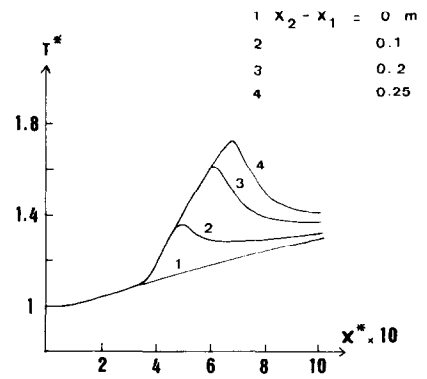

FIG. 10. Effect of the dry zone length on the local dimensionless temperature for $y = 3$ mm: forced convection case. $T_\infty = 298$ K; $q = 300$ W m^{-2}; $C_\infty = 0.008$ kg kg^{-1} (dry basis); $U_\infty = 2$ m s^{-1}; $L = 1$ m.

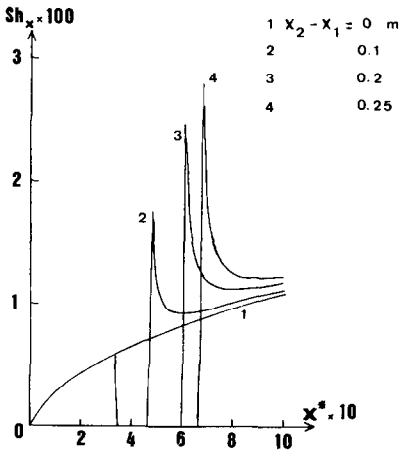

FIG. 9. Effect of the dry zone length on the local Sherwood number: forced convection case. $T_\infty = 298$ K; $q = 300$ W m^{-2}; $C_\infty = 0.008$ kg kg^{-1} (dry basis); $U_\infty = 2$ m s^{-1}; $L = 1$ m.

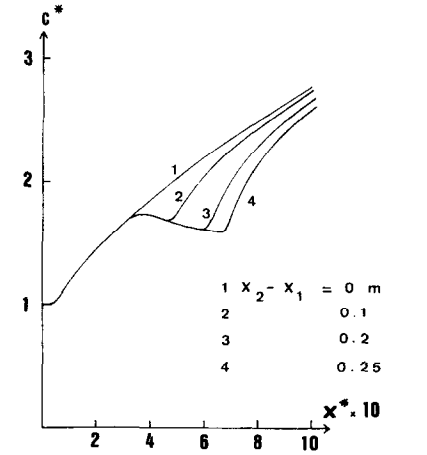

FIG. 11. Effect of the dry zone length on the local dimensionless vapour concentration for $y = 3$ mm: forced convection case. $T_\infty = 298$ K; $q = 300$ W m^{-2}; $C_\infty = 0.008$ kg kg^{-1} (dry basis); $U_\infty = 2$ m s^{-1}; $L = 1$ m.

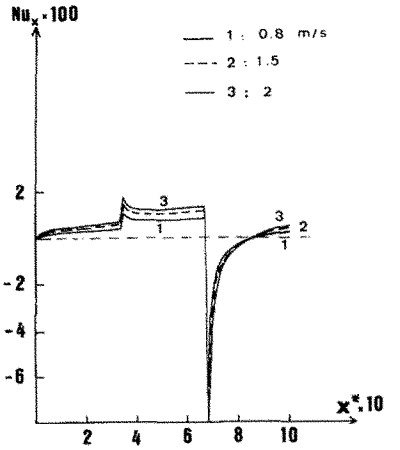

FIG. 12. Effect of the free stream velocity on the local Nusselt number: forced convection case. $T_\infty = 298$ K; $q = 300$ W m^{-2}; $C_{v\infty} = 0.008$ kg kg^{-1} (dry basis).

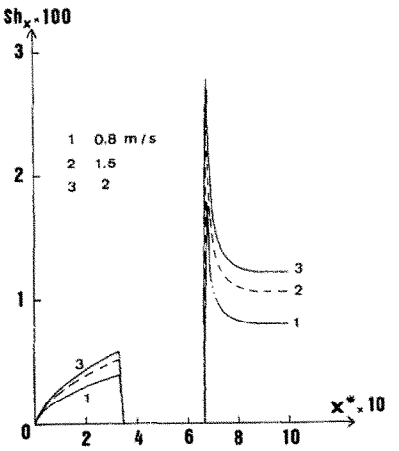

FIG. 13. Effect of the free stream velocity on the local Sherwood number: forced convection case. $T_\infty = 298$ K; $q = 300$ W m^{-2}; $C_{v\infty} = 0.008$ kg kg^{-1} (dry basis).

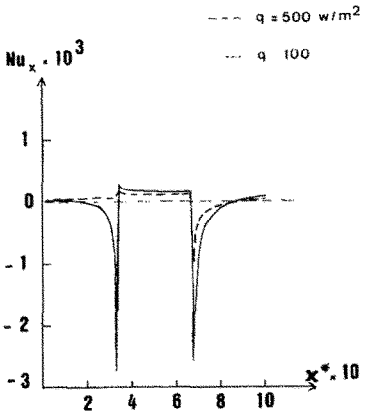

FIG. 14. Effect of the incident wall heat flux density on the local Nusselt number: forced convection case. $T_\infty = 298$ K; $U_\infty = 2$ m s^{-1}; $C_{v\infty} = 0.008$ kg kg^{-1} (dry basis).

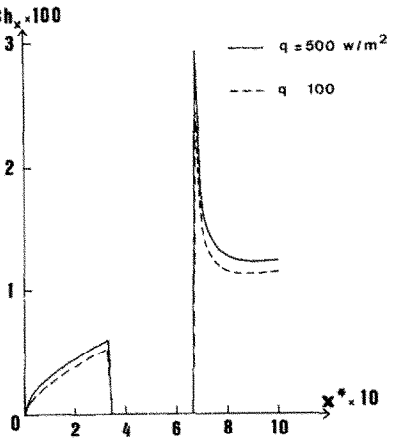

FIG. 15. Effect of the incident wall heat flux density on the local Sherwood number: forced convection case. $T_\infty = 298$ K; $U_\infty = 2$ m s^{-1}; $C_{v\infty} = 0.008$ kg kg^{-1} (dry basis).

and it follows that the negative value of the Nusselt number for $x = x_2$ decreases as U_∞ increases.

The effect of the density of the incident wall heat flux, q, on the local Nusselt and Sherwood numbers is shown in Figs. 14 and 15, respectively. From the variations of the local Sherwood number, it is clear that the evaporation rate increases as the incident wall heat flux increases. At the same time, for low values of q ($q = 100$ W m^{-2}), the local Nusselt number first slightly increases up to $x^* \simeq 0.1$ and then decreases and becomes negative for $x^* \simeq 0.2$. Indeed, from this value and up to the separation zone between the first wet region and the dry one, the wall temperature becomes lower than the temperature of the drying air because of the increase of wall cooling by the evaporation process. In the dry zone, the wall temperature again increases because there is no longer evaporation and the Nusselt number also increases and becomes positive with a larger value than for $q = 500$ W m^{-2}, since the wall temperature gradient also increases.

4.2. *Free convection case*

For the free convection case, typical profiles of the local Nusselt and Sherwood numbers are respectively shown in Figs. 16 and 17 and they are seen to be very similar to the forced convection case. As for Figs. 5 and 6, the lengths of the dry zone and the two wet zones are equal. In Fig. 18, the variation of the corresponding local wall shear stress is reported: because $\varepsilon = 1$, the momentum equation is now coupled with the energy and mass diffusion equations, so that the velocity and its first derivative are highly correlated with the buoyancy thermal and mass forces. For $x^* > x_1^*$, the wall temperature increases with an accompanying increase of the buoyancy thermal force, as compared with the first wet zone. It follows that the drying air is accelerated along the dry region and the wall shear stress also increases before suddenly decreasing for $x = x_2^*$. The dimensionless

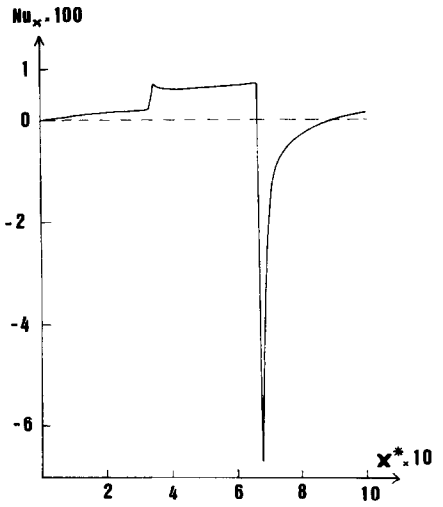

FIG. 16. Variation of the local Nusselt number: free convection case. $T_\infty = 293$ K; $q = 200$ W m^{-2}; $C_\infty = 0.008$ kg kg^{-1} (dry basis); $\alpha = 45°$.

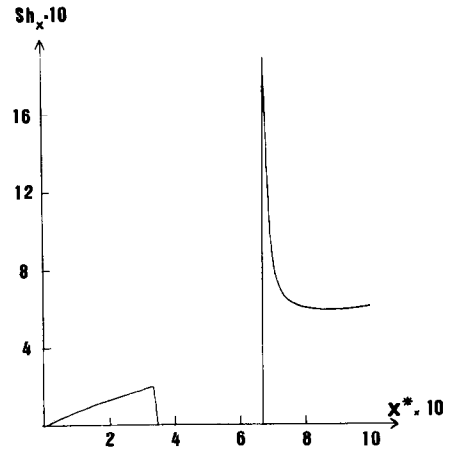

FIG. 17. Variation of the local Sherwood number: free convection case. $T_\infty = 293$ K; $q = 200$ W m^{-2}; $C_\infty = 0.008$ kg kg^{-1} (dry basis); $\alpha = 45°$.

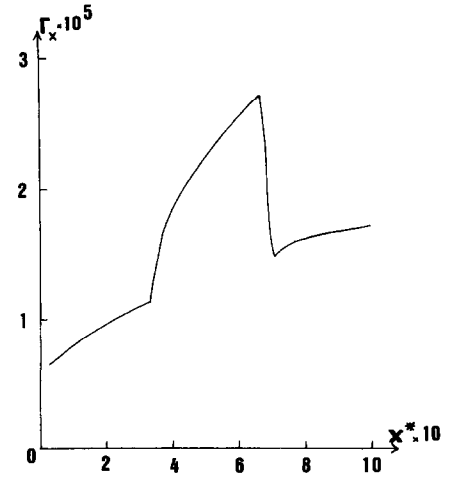

FIG. 18. Variation of the local wall shear stress: free convection case. $T_\infty = 293$ K; $q = 200$ W m^{-2}; $C_\infty = 0.008$ kg kg^{-1} (dry basis); $\alpha = 45°$.

x^*-velocity, temperature and vapour concentration profiles are drawn in Figs. 19–21, respectively. Figure 19 clearly shows the fluid acceleration which occurs near the wall in the dry zone.

Figures 22 and 23 illustrate the effect of the inclination angle from the vertical plane on the local Nusselt and Sherwood numbers: in the momentum equation, the intensity of the buoyancy forces diminishes as this angle increases, so that the heat and mass transfer coefficients also decrease. These results agree with others which are reported in the literature [5] and it can be concluded that the inclination angle is not an essential criterion. On the other hand, the velocity, temperature and vapour concentration profiles are highly affected by the length of the dry zone, as for the forced convection case. Figures 24 and 25 show

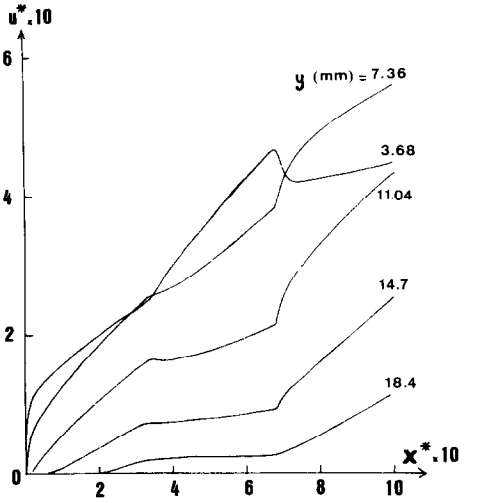

FIG. 19. Dimensionless x^*-velocity profiles in the boundary layer: free convection case. $T_\infty = 293$ K; $q = 200$ W m^{-2}; $C_\infty = 0.008$ kg kg^{-1} (dry basis); $\alpha = 45°$.

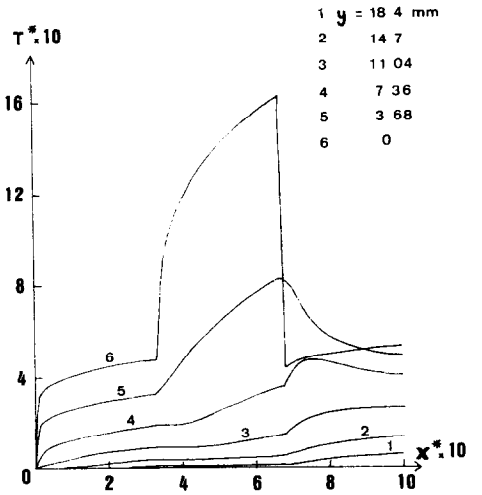

FIG. 20. Dimensionless local temperature profiles in the boundary layer: free convection case. $T_\infty = 293$ K; $q = 200$ W m^{-2}; $C_\infty = 0.008$ kg kg^{-1} (dry basis); $\alpha = 45°$.

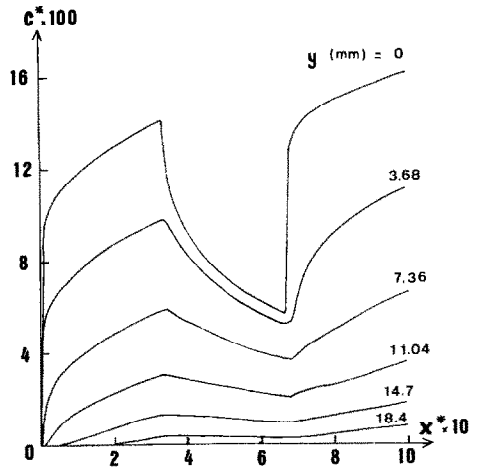

FIG. 21. Dimensionless local vapour concentration profiles in the boundary layer: free convection case. $T_\infty = 293$ K; $q = 200$ W m^{-2}; $C_\infty = 0.008$ kg kg^{-1} (dry basis); $\alpha = 45°$.

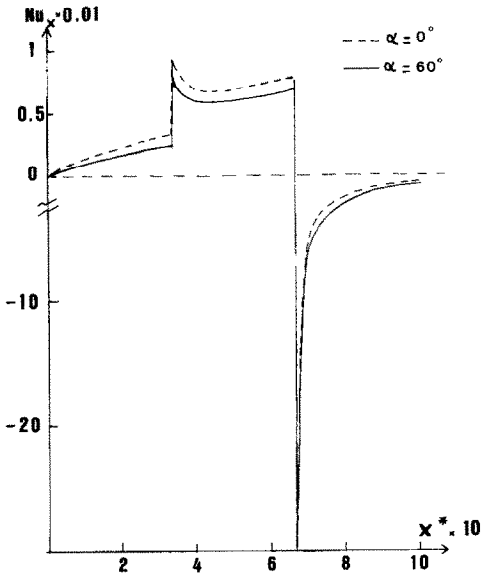

FIG. 22. Variation of the local Nusselt number as a function of the inclination angle α: free convection case. $T_\infty = 298$ K; $q = 200$ W m^{-2}; $C_\infty = 0.001$ kg kg^{-1} (dry basis).

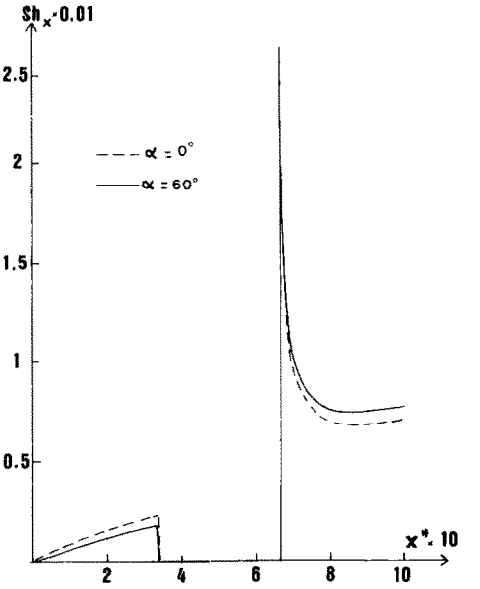

FIG. 23. Variation of the local Sherwood number as a function of the inclination angle α: free convection case. $T_\infty = 298$ K; $q = 200$ W m^{-2}; $C_\infty = 0.001$ kg kg^{-1} (dry basis).

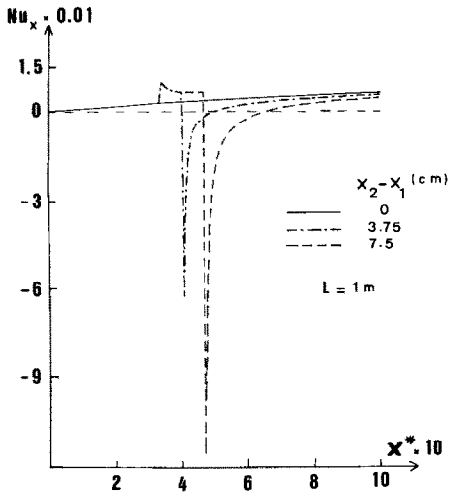

FIG. 24. Variation of the local Nusselt number as a function of the dry zone length: free convection case. $T_\infty = 298$ K; $q = 200$ W m^{-2}; $C_\infty = 0.001$ kg kg^{-1} (dry basis); $\alpha = 45°$; $L = 1$ m.

this effect on the local Nusselt and Sherwood numbers. It is seen that the larger the length $(x_2 - x_1)$, the better the mass transfer rate along the last wet region, which is due to the increase of the wall temperature at the end of the dry zone.

5. CONCLUSION

The laminar heat and mass transfer from an inclined flat plate with a dry zone inserted between two wet zones has been studied. Appropriate mathematical transformations allowed us to obtain the same dimensionless system of equations in order to study both free and forced convection cases. These equations were solved by using an adaptation of the Nogotov procedure. The effects of the main physical parameters on the velocity, temperature and vapour concentration profiles in the boundary layer have been examined and the resulting local Nusselt and Sherwood numbers have been determined. From the results, it appears that the length of the central dry region is an essential criterion.

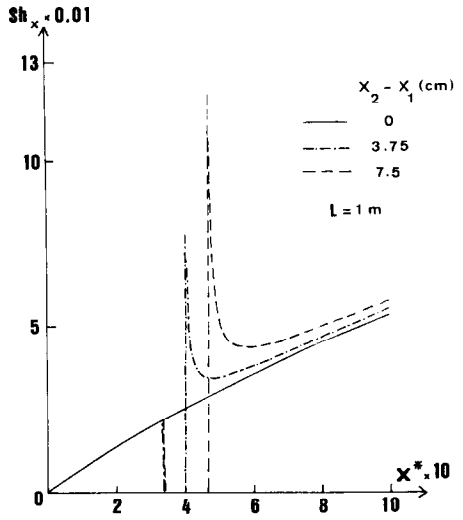

FIG. 25. Variation of the local Sherwood number as a function of the dry zone length: free convection case. $T_\infty = 298$ K; $q = 200$ W m^{-2}; $C_\infty = 0.001$ kg kg^{-1} (dry basis); $\alpha = 45°$; $L = 1$ m.

REFERENCES

1. W. M. Roshenow, J. P. Harnett and E. N. Ganic, *Handbook of Heat Transfer*, 2nd Edn. McGraw-Hill, New York (1985).
2. H. Schlichting, *Boundary Layer Theory*, 6th Edn. McGraw-Hill, New York (1968).
3. T. S. Chen and C. F. Yuh, Combined heat and mass transfer in natural convection on inclined surfaces, *Numer. Heat Transfer* **2**, 233–250 (1979).
4. T. S. Chen, H. C. Tien and B. F. Armaly, Natural convection on horizontal, inclined and vertical plates with variable surface temperature or heat flux, *Int. J. Heat Mass Transfer* **29**, 1465–1478 (1986).
5. B. Zeghmati, G. Le Palec and M. Daguenet, Study of transient laminar free convection over an inclined wet flat plate, *Int. J. Heat Mass Transfer* **34**, 899–909 (1991).
6. M. Mammou, Etude des transferts simultanés d'impulsion, de chaleur et de masse au-dessus d'une paroi solide formée de deux zones humides séparées par une zone sèche, Thesis, Perpignan (1990).
7. G. Bruhat, *Thermodynamique*, 6th Edn. Masson, Paris (1968).
8. J. F. Sacadura, *Initiation aux Transferts Thermiques*. CAST, Techniques et documentation, Paris (1978).
9. E. N. Nogotov, *Application of Numerical Heat Transfer*. McGraw-Hill, New York (1978).
10. D. A. Anderson, J. C. Tannhill and R. H. Fletcher, *Computational Fluid Mechanics and Heat Transfer*. Hemisphere, Washington (1984).
11. J. M. Varah, On the solution of block-tridiagonal systems arising from certain finite-difference equations, *Math. Comput.* **26**(120), 859–868 (1972).
12. G. S. Callahan and W. J. Marner, Transient free convection with mass transfer on an isothermal vertical flat plate, *Int. J. Heat Mass Transfer* **19**, 165–174 (1976).
13. F. A. Bottemane, Theoretical solution of simultaneous heat and mass transfer by free convection about vertical flat plate, *Appl. Sci. Res.* **25**, 137–149 (1971).
14. B. Gebhart and L. Pera, The nature of vertical natural convection flow resulting from the combined buoyancy effects of thermal and mass diffusion, *Int. J. Heat Mass Transfer* **14**, 2025–2050 (1971).
15. M. Vachon, Etude de l'évaporation en convection naturelle, Thesis, Poitiers (1979).

ETUDE NUMERIQUE DU TRANSFERT DE MASSE ET DE CHALEUR SUR UNE PLAQUE PLANE INCLINEE, CONSTITUEE DE ZONES SECHES ET HUMIDES

Résumé—Cet article présente une étude théorique des transferts d'impulsion, de masse et de chaleur dans la couche limite laminaire qui si développe par convection forcée ou naturelle au-dessus d'une plaque plane inclinée lorsqu'elle est soumise à un flux de densité constante. Cette plaque est constituée de deux zones humides qui encadrent une zone sèche. Les équations sont adimensionnalisées et le système différentiel qui en résulte est résolu par une méthode implicite aux différences finies. Les résultats mettent en évidence l'influence des principaux paramètres sur les profils de vitesse, de température et de concentration dans la couche limite: en particulier, la longueur de la zone sèche joue un rôle essentiel.

NUMERISCHE UNTERSUCHUNG DER WÄRME- UND STOFFÜBERTRAGUNG AN EINER GENEIGTEN PLATTE MIT NASSEN UND TROCKENEN GEBIETEN

Zusammenfassung—In der vorliegenden Arbeit wird die Impuls-, Wärme- und Stoffübertragung in der laminaren Grenzschicht untersucht, die sich entlang einer geneigten ebenen Platte bei freier oder erzwungener Konvektion mit konstanter Wärmestromdichte an der Wand ausbildet. Die Platte besteht aus zwei nassen Zonen, die durch eine trockene Zone getrennt sind. Aus der theoretischen Analyse ergibt sich ein System dimensionsloser gekoppelter Gleichungen, das mit Hilfe eines impliziten Finite-Differenzen Verfahrens gelöst wird. Die Ergebnisse zeigen den Einfluß der meisten physikalischen Grundgrößen auf Geschwindigkeits-, Temperatur- und Konzentrationsprofile in der Grenzschicht. Aufgrund dieser Untersuchung scheint die Länge der trockene Trennungszone ein grundlegendes Kriterium zu sein.

ЧИСЛЕННЫЙ АНАЛИЗ ТЕПЛО-И МАССОПЕРЕНОСА ОТ НАКЛОННОЙ ПОЛОСКОЙ ПЛАСТИНЫ ПРИ НАЛИЧИИ ВЛАЖНОЙ И СУХОЙ ЗОН

Аннотация—Теоретически исследуется перенос импульса, тепла и массы в ламинарном пограничном слое, развивающийся над наклонной плоской пластиной под действием свободной или вынужденной конвекций в случае постоянного заданного теплового потока на стенке. Пластина изготовлена таким образом, что на ней присутствуют две влажные зоны, разделенные сухой. Выведенная из теоретического анализа система взаимосвязанных безразмерных уравнений решается численно с помощью неявного метода конечных разностей. Результаты иллюстрируют влияние большинства основных физических величин на профили скоростей, температур и концентраций в пограничном слое. Из данной работы следует, что длина сухой разделяющей зоны является определяющим критерием.